



HAL
open science

Multi-objective qLPV Hinf / H2 Control of a half vehicle

Charles Poussot-Vassal, Olivier Sename, Luc Dugard, Peter Gaspar, Zoltan Szabo, Jozsef Bokor

► **To cite this version:**

Charles Poussot-Vassal, Olivier Sename, Luc Dugard, Peter Gaspar, Zoltan Szabo, et al.. Multi-objective qLPV Hinf / H2 Control of a half vehicle. 10th Mini Conference on vehicle system dynamics, identification and anomalies, VSDIA, 2006, Budapest, Hungary. hal-00098656

HAL Id: hal-00098656

<https://hal.science/hal-00098656>

Submitted on 26 Oct 2007

HAL is a multi-disciplinary open access archive for the deposit and dissemination of scientific research documents, whether they are published or not. The documents may come from teaching and research institutions in France or abroad, or from public or private research centers.

L'archive ouverte pluridisciplinaire **HAL**, est destinée au dépôt et à la diffusion de documents scientifiques de niveau recherche, publiés ou non, émanant des établissements d'enseignement et de recherche français ou étrangers, des laboratoires publics ou privés.

Multi-objective qLPV $\mathcal{H}_\infty/\mathcal{H}_2$ control of a half vehicle

C. Poussot-Vassal¹, O. Sename¹, L. Dugard¹, P. Gáspár², Z. Szabó², J. Bokor²

Abstract—In this paper we compare LTI and qLPV $\mathcal{H}_\infty/\mathcal{H}_2$ controllers. The Pareto limit is used to show the compromise that has to be done when a mixed synthesis is achieved. Simulations on a nonlinear half vehicle model, with multiple objectives, are performed to show the efficiency of the method.

Index Terms—Half vehicle, LMI based multi-objective synthesis, qLPV systems, Mixed qLPV polytopic $\mathcal{H}_\infty/\mathcal{H}_2$ control, Pareto limit.

I. INTRODUCTION

The main role of suspensions is to improve comfort by isolating the vehicle chassis to an uneven ground and to provide a good road holding to ensure passenger safety. Suspension control of quarter vehicle have been widely explored the past few years to improve vertical movements either by applying LQ [9], Skyhook [11], \mathcal{H}_∞ control [7], [16], LPV [4] or mixed synthesis [1], [14]. Roll dynamic is caught by the half vehicle model and is directly linked to suspension behavior. Separated synthesis on each suspension can't guarantee global performances. The aim of the mixed $\mathcal{H}_\infty/\mathcal{H}_2$ control synthesis is to treat the standard \mathcal{H}_2 and \mathcal{H}_∞ optimal control problems as separate problems but in a unified state-space framework. This method yields a compensator that combines the \mathcal{H}_2 quadratic performance criterion for disturbance rejection with the \mathcal{H}_∞ performance criterion for maximum robustness against destabilizing uncertainties. It means, the controller which minimizes the \mathcal{H}_2 performance index is selected from the suitable \mathcal{H}_∞ controllers, thus the desired criteria are met by creating a balance between \mathcal{H}_2 and \mathcal{H}_∞ norms [3].

The mixed qLPV $\mathcal{H}_\infty/\mathcal{H}_2$ method is proposed here for the design of active suspension system, in which different optimization criteria are applied to guarantee the performance specifications and the nonlinearity of the suspension system. The nonlinearity in the suspension system is caused by the changes in the spring and damping coefficients. It is assumed that the nonlinear dynamics of road vehicles is approximated by LPV (qLPV) models, in which nonlinear terms are hidden with newly defined scheduling variables and they are available from calculated signals. The active suspension based on the LPV model takes the nonlinear dynamics of the system into consideration. Performance

limitations according to the importance given between the \mathcal{H}_∞ and the \mathcal{H}_2 criteria is shown with the Pareto limit.

The paper is organized as follows: in Section II we introduce a linear and a nonlinear model of the half vehicle. LTI and qLPV polytopic $\mathcal{H}_\infty/\mathcal{H}_2$ control, based on LMIs, are presented in Section III. The Pareto limit, applied to the half vehicle provides smart indications in the way to choose $\mathcal{H}_\infty/\mathcal{H}_2$ attenuation parameters according to the desired performances. In Section IV, validations are done on the nonlinear model presented.

II. HALF VEHICLE MODEL

A. Model description

Roll dynamic is the main movement that enters when a driver turns. The half vehicle model involved here is a chassis model that catches vertical and roll dynamics [11] (Figure 1). It models the left/right vehicle load transfers that appears during a steering situation. The model is composed of two suspensions, each of them modeled by a spring ($F_{k_{\{fl,fr\}}}$), a damper ($u_{\{fl,fr\}} = F_{c_{\{fl,fr\}}}$, in the passive case) or an actuator ($u_{\{fl,fr\}} = u_{\{fl,fr\}}^{\mathcal{H}_\infty/\mathcal{H}_2} + c_{\{fl,fr\}}$, in the active case) linked to a common suspended mass (m_s) and to a specific unsprung mass $m_{us_{fl}}$ and $m_{us_{fr}}$. Tires $k_{t_{fl}}$ and $k_{t_{fr}}$ are linked to the ground and to the unsprung mass $m_{us_{fl}}$ and $m_{us_{fr}}$, respectively. Note that $u_{\{fl,fr\}}^{\mathcal{H}_\infty/\mathcal{H}_2}$ comes from the controller synthesized in Section III.

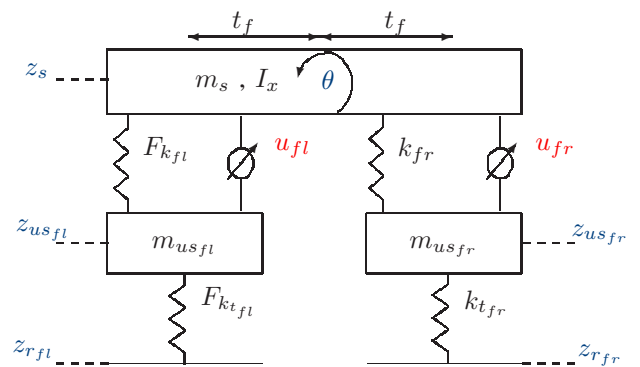


Fig. 1. Half vehicle model

The movements taken into account are the vertical displacement of the suspended mass (z_s), the unsprung masses ($z_{us_{\{fl,fr\}}}$), the suspension deflections ($z_{def_{\{fl,fr\}}}$) and the roll angle (θ) of the center of gravity of the suspended mass. The nonlinear effects of the actuator dynamics are ignored for simplicity.

¹ Laboratoire d'Automatique de Grenoble, ENSIEG - Domaine Universitaire - BP46, 38402 Saint Martin d'Hères - Cedex FRANCE, e-mail : {charles.poussot, olivier.sename, luc.dugard}@lag.ensieg.inpg.fr

² Computer and Automation Research Institute, Hungarian Academy of Sciences, Kende u. 13-17, H-1111, Budapest, HUNGARY, e-mail : {gaspar,szabo,bokor}@sztaki.hu

B. Model dynamical equations

The model is obtained by simply adding two suspensions and tires equations with the dynamical equation of the chassis as follows. First we derive the suspension (F_{sz_i}) and tire (F_{tz_i}) forces,

$$\begin{cases} F_{tz_{fl}} &= k_{t_{fl}}(z_{us_{fl}} - z_{r_{fl}}) \\ F_{tz_{fr}} &= k_{t_{fr}}(z_{us_{fr}} - z_{r_{fr}}) \\ F_{sz_{fl}} &= F_{k_{fl}}(z_{s_{fl}} - z_{us_{fl}}) - \frac{k_b \theta}{2l_{fl}} + u_{fl} \\ F_{sz_{fr}} &= F_{k_{fr}}(z_{s_{fr}} - z_{us_{fr}}) + \frac{k_b \theta}{2l_{fr}} + u_{fr} \end{cases}$$

where,

$$\begin{cases} z_{s_{fl}} &= z_s - t_f \sin(\theta) \\ z_{s_{fr}} &= z_s + t_f \sin(\theta) \\ \dot{z}_{s_{fl}} &= \dot{z}_s - \dot{\theta} t_f \cos(\theta) \\ \dot{z}_{s_{fr}} &= \dot{z}_s + \dot{\theta} t_f \cos(\theta) \end{cases}$$

then the dynamic of the chassis and unsprung masses (bounce and roll) are given by,

$$\begin{cases} m_s \ddot{z}_s &= -(F_{sz_{fl}} + F_{tz_{fr}} + F_{dz}) \\ m_{us_{fl}} \ddot{z}_{us_{fl}} &= F_{sz_{fl}} - F_{tz_{fl}} \\ m_{us_{fr}} \ddot{z}_{us_{fr}} &= F_{sz_{fr}} - F_{tz_{fr}} \\ I_x \ddot{\theta} &= F_{sz_{fl}} t_f - F_{tz_{fr}} t_f + M_{dx} \end{cases} \quad (1)$$

where F_{k_i} and F_{c_i} , $\{i = fl, fr\}$, represent the force delivered by the spring and by the damper (either linear or nonlinear), k_{t_i} is the stiffness of the tire and k_b models the influence of an anti-roll bar. I_x is the chassis inertia on the roll axis, t_f is the distances of the unsprung masses to the center of gravity of the suspended mass (table I). Finally, θ , z_s , $z_{us_{fl}}$ and $z_{us_{fr}}$ represent the roll angle and the chassis, unsprung mass left and right bounce. Then $z_{r_{fl}}$ and $z_{r_{fr}}$ represent the road disturbances on the wheels. F_{dz} , M_{dx} represent the load and inertia disturbances. Note that when the passive system is considered, $u_{fr} = F_{c_{fr}}$ and $u_{fl} = F_{c_{fl}}$.

Then, the state space vector of the linear model is defined by $x = [z_{us_{fl}} \ \dot{z}_{us_{fl}} \ z_{us_{fr}} \ \dot{z}_{us_{fr}} \ z_s \ \dot{z}_s \ \theta \ \dot{\theta}]$, the input are given by $w = [z_{r_{fl}} \ z_{r_{fr}} \ F_{dz} \ M_{dx} \ u_{fl} \ u_{fr}]$ and the measured signal used for control $y = [z_{def_{fl}} \ z_{def_{fr}}]$.

Symbol	Value	Description
m_s	$315 \times 2 \text{ kg}$	sprung mass
$m_{us_{fl}}, m_{us_{fr}}$	37.5 kg	unsprung masses
k_{fl}, k_{fr}	29500 N/m	suspensions linearized stiffness
c_{fl}, c_{fr}	1500 N/m/s	suspensions linearized damping
$k_{t_{fl}}, k_{t_{fr}}$	208000 N/m	tires stiffness
I_x	250 kg.m^2	sprung mass inertia
l_f	1.2 m	distance to the center of gravity
k_b	150000 N/m	anti-roll bar (if any)

TABLE I
PARAMETERS OF THE MODEL

In the nonlinear model, we assume that the spring (F_{k_i}) and the damper (F_{c_i}) forces are nonlinear functions of z_{def_i} and \dot{z}_{def_i} respectively [15] (Figure 2). For all the simulations we will consider the nonlinear model.

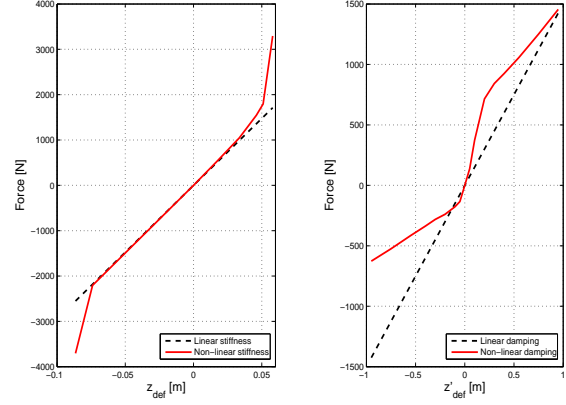


Fig. 2. Linear (dashed) vs. Non-Linear (solid) stiffness (left) and damping (right) coefficient

Figure 3 compares frequency behavior of the linear model with the nonlinear one. The frequency plots of the nonlinear model are made assuming a sinusoidal input z_r of magnitude 10cm over 10 periods (with varying frequency) and by calculation of the discrete Fourier Transform to evaluate the system gain.

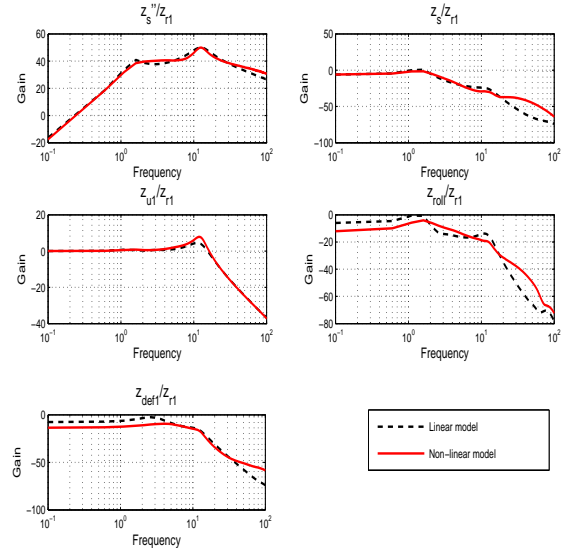


Fig. 3. Linear (dashed) vs. Non-Linear (solid) half vehicle model open loop frequency behavior

III. MIXED $\mathcal{H}_\infty / \mathcal{H}_2$ LMI BASED SYNTHESIS

A. A LTI multi-objective controller

The multi-objective synthesis consists of giving different kind of constraints on the output of a system. With this formulation (for the case of $\mathcal{H}_\infty / \mathcal{H}_2$), let describe the system

as follows

$$\begin{bmatrix} \dot{x} \\ z_\infty \\ z_2 \\ y \end{bmatrix} = \begin{bmatrix} A & B_\infty & B_2 & B \\ C_\infty & D_{\infty 1} & D_{\infty 2} & E_\infty \\ C_2 & D_{21} & D_{22} & E_2 \\ C & F_\infty & F_2 & 0 \end{bmatrix} \begin{bmatrix} x \\ w_\infty \\ w_2 \\ u \end{bmatrix} \quad (2)$$

the controller,

$$\begin{bmatrix} \dot{x}_c \\ u \end{bmatrix} = \begin{bmatrix} A_c & B_c \\ C_c & D_c \end{bmatrix} \begin{bmatrix} x \\ y \end{bmatrix} = S \quad (3)$$

and the closed loop,

$$\begin{bmatrix} \dot{x} \\ z_\infty \\ z_2 \end{bmatrix} = \begin{bmatrix} A & B_\infty & B_2 \\ C_\infty & D_{\infty 1} & D_{\infty 2} \\ C_2 & D_{21} & 0 \end{bmatrix} \begin{bmatrix} x \\ w_\infty \\ w_2 \end{bmatrix} \quad (4)$$

The $\mathcal{H}_\infty / \mathcal{H}_2$ synthesis consists of, imposing $T_\infty = \|z_\infty/w_\infty\|_\infty < \gamma_\infty$ and $T_2 = \|z_2/w_2\|_2 < \gamma_2$. Hence the LMI based problem formulation is the following: minimize γ_2 and γ_∞ subject to K and Z . [2], [12]

$$\begin{cases} \begin{bmatrix} A^T K + K A & K B_\infty & C_\infty^T \\ B_\infty^T K & -\gamma_\infty^2 I & D_{\infty 1}^T \\ C_\infty & D_{\infty 1} & -I \end{bmatrix} < 0 \\ \begin{bmatrix} A^T K + K A & K B_2 \\ B_2^T K & -I \end{bmatrix} < 0, \\ \begin{bmatrix} K & C_2^T \\ C_2 & Z \end{bmatrix} > 0, \\ \text{Trace}(Z) < \gamma_2, D_{22} = 0 \end{cases} \quad (5)$$

Then solving this problem gives the LTI controller that achieves the desired performances. Note that to relax BMIs (5) into LMIs we use the transformation given in [12].

B. A qLPV multi-objective controller

Linear parameter varying theory is useful to tackle measurable and bounded nonlinearities. We talk about qLPV when the varying parameters only enter in the dynamic matrix A of the system. In the suspension system, the measure of the deflection (used as a controller input) can also be used to reconstruct the stiffness coefficient [16]. To build a qLPV controller, we use the polytopic approach which consists of building a controller to the k -corners of the polytope (formed by all the possible combinations of the upper and lower bounds of each varying parameters) and to schedule these k -controllers by the measure of the varying variables [6], [8]. The qLPV system is described as follows, with p a varying parameter,

$$\begin{bmatrix} \dot{x} \\ z_\infty \\ z_2 \\ y \end{bmatrix} = \begin{bmatrix} A(p) & B_\infty & B_2 & B \\ C_\infty & D_{\infty 1} & D_{\infty 2} & E_\infty \\ C_2 & D_{21} & D_{22} & E_2 \\ C & F_\infty & F_2 & 0 \end{bmatrix} \begin{bmatrix} x \\ w_\infty \\ w_2 \\ u \end{bmatrix} \quad (6)$$

the parameter dependent controller,

$$\begin{bmatrix} \dot{x}_c \\ u \end{bmatrix} = \begin{bmatrix} A_c(p) & B_c(p) \\ C_c(p) & D_c(p) \end{bmatrix} \begin{bmatrix} x_c \\ y \end{bmatrix} = S(p) \quad (7)$$

and the parameter dependent closed loop,

$$\begin{bmatrix} \dot{x} \\ z_\infty \\ z_2 \end{bmatrix} = \begin{bmatrix} A(p) & B_\infty & B_2 \\ C_\infty & D_{\infty 1} & D_{\infty 2} \\ C_2 & D_{21} & 0 \end{bmatrix} \begin{bmatrix} x \\ w_\infty \\ w_2 \end{bmatrix} \quad (8)$$

Then the corresponding mixed problem is similar to the LTI one: minimize γ_2 and γ_∞ subject to K and Z .

$$\begin{cases} \begin{bmatrix} A(p)^T K + K A(p) & K B_\infty & C_\infty^T \\ B_\infty^T K & -\gamma_\infty^2 I & D_{\infty 1}^T \\ C_\infty & D_{\infty 1} & -I \end{bmatrix} < 0 \\ \begin{bmatrix} A(p)^T K + K A(p) & K B_2 \\ B_2^T K & -I \end{bmatrix} < 0, \\ \begin{bmatrix} K & C_2^T \\ C_2 & Z \end{bmatrix} > 0, \\ \text{Trace}(Z) < \gamma_2, D_{22} = 0 \end{cases} \quad (9)$$

The polytopic approach consists of finding a common Lyapunov function K and a γ_∞, γ_2 and Z that solve the previous LMIs (9) problem at each corners of the polytope. Then the control to apply is a convex combination of these k -controllers expressed as follows,

$$S(p) = \sum_{k=1}^{2^i} \alpha_k(p) \begin{bmatrix} A_{c_k} & B_{c_k} \\ C_{c_k} & D_{c_k} \end{bmatrix}$$

where,

$$\alpha_k(p) = \frac{\prod_{j=1}^i |p(j) - \text{compl}(\text{coin}\Theta_k)_j|}{\prod_{j=1}^i (\bar{p}(j) - \underline{p}(j))},$$

and,

$$\sum_{k=1}^{2^i} \alpha_k(p) = 1, \alpha_k(p) > 0$$

where i is the number of varying parameters and $k = 2^i$, the number of corners of the polytope. Let note \bar{p} and \underline{p} the upper and lower bounds of a parameter respectively. Finally, $\text{compl}(\text{coin}\Theta_k)$ represents the complementary of Θ_k , which is simply the k^{th} corner of the polytope [15].

C. Design characteristics and performances on the half vehicle model

In the case of a half vehicle, the measure is the suspension deflection and the selected varying variables are the stiffness of the suspension spring, i.e. k_{fl} and k_{fr} . The associated polytope is then formed by $k = 4$ corners (10) and k -controllers.

$$\Theta = \begin{bmatrix} \underline{k}_{fl} & \underline{k}_{fr} \\ \underline{k}_{fl} & \bar{k}_{fr} \\ \bar{k}_{fl} & \underline{k}_{fr} \\ \bar{k}_{fl} & \bar{k}_{fr} \end{bmatrix}, \quad \begin{matrix} k_{fl} \in [\underline{k}_{fl}, \bar{k}_{fl}] \\ k_{fr} \in [\underline{k}_{fr}, \bar{k}_{fr}] \end{matrix} \quad (10)$$

According to the dissipative theory, each constraint can be expressed as a supply function, then translated into an LMI (5, 9) [12], [13].

- The \mathcal{H}_∞ performance is used to enforce robustness to model uncertainties and to express frequency-domain performance specifications
- The \mathcal{H}_2 performance can be used to minimize energy of the signal (note the equivalence of these norms in the frequency domain, but not in the time one)

Hence, coupled together, these specifications should improve the single \mathcal{H}_∞ constraint. On a half vehicle model the performances we want to reach are multiple. As exposed in [10], [11], some frequency specifications have to be specified concerning the suspension deflection, suspended mass and the unsprung masses (to reduce gain around sensitive low frequencies). Also, weight on the control signal prevent actuator saturation. To these frequency specifications, expressed by the \mathcal{H}_∞ theory, the addition of \mathcal{H}_2 constrain is used to minimize energy of time signals. Hence, the applied weights can be the following,

$$\begin{cases} W_{z_s} &= 5 \frac{1}{1/(2\pi 5)s+1} \\ W_\theta &= \frac{1}{1/(2\pi)s+1} \\ W_{u_{\{fl,fr\}}} &= 2.10^{-3} \\ W_{zr_{\{fl,fr\}}} &= 0.07 \\ W_{n_{\{fl,fr\}}} &= 0.001 \end{cases}$$

Then, the resulting generalized plant is (Figure 4),

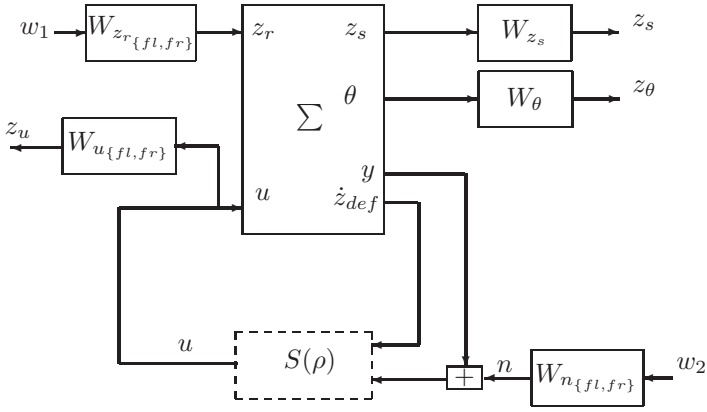


Fig. 4. Generalized plant

In the mixed synthesis the considered \mathcal{H}_∞ and \mathcal{H}_2 controlled output, noted z_∞ and z_2 respectively, are the following,

$$\begin{aligned} z_\infty &= \begin{bmatrix} z_s & z_\theta & z_{u_{fl}} & z_{u_{fr}} \end{bmatrix} \\ z_2 &= \begin{bmatrix} z_s & z_\theta & z_{u_{fl}} & z_{u_{fr}} \end{bmatrix} \end{aligned}$$

Note that when we will compare the mixed synthesis to the \mathcal{H}_∞ one, the controlled outputs of the \mathcal{H}_∞ controller are, $z_\infty = [z_s \ z_\theta \ z_{u_{fr}} \ z_{u_{fl}}]$.

D. Pareto limit

It is impossible to minimize both γ_∞ and γ_2 . In the literature, the mixed problem is generally solved by minimizing a convex combination of \mathcal{H}_∞ and \mathcal{H}_2 that represents a compromise between the two performances. Such a minimization can take the following form,

$$\min\{\alpha_1 T_\infty + \alpha_2 T_2\},$$

where $\{\alpha_1, \alpha_2\} \in [0, 1] \times [0, 1], \alpha_1 + \alpha_2 = 1$

Hence a natural problem raises, how to choose in a smart way α_1 and α_2 . The concept of non-inferiority (also called

Pareto optimality) is used here to characterize the objectives. A non-inferior solution is one in which an improvement in one objective requires a degradation of an other. In our case the objectives are \mathcal{H}_∞ and \mathcal{H}_2 . To plot the Pareto optimum, applied to our problem, we iteratively fix the γ_∞ and minimize the γ_2 . The corresponding results are given in Figure 5.

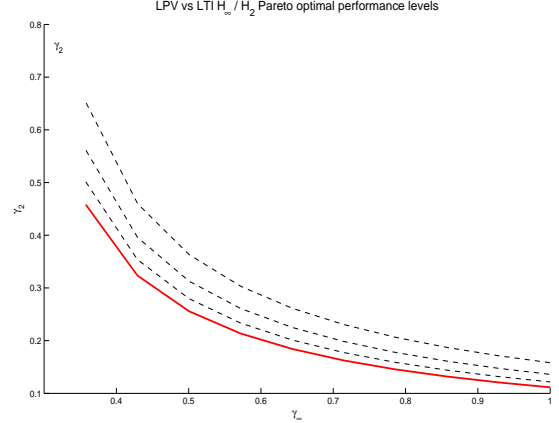


Fig. 5. LTI (solid) vs qLPV (dashed) Pareto limit for $k_{\{fl,fr\}} \in k_{nom} \times [1, 1.2], [1, 1.5], [1, 2]$

The achievable combinations $\{\gamma_\infty, \gamma_2\}$ is the set of couples located over the Pareto limit. The Pareto limit is also useful to measure the conservatism of a method and to exhibit how much one can decrease the performances with a qLPV approach compared to the LTI one. Such a Figure can also motivate researches on polytope reduction. In effect, the more you increase the size of your polytope (bounds of the parameters), the more far you go from the LTI Pareto optimum (Figure 5), and loose performance.

IV. SIMULATION RESULTS

To validate the control design, first, simulations are done in order to show the advantages of mixed synthesis compared to single \mathcal{H}_∞ objective, then, we study the influence of the choice of the couple $\{\gamma_\infty, \gamma_2\}$ on the reached performances. Finally, we compare the LTI mixed approach with the qLPV one. Note that on these simulations, when a control law is considered, the damper is removed so that the considered suspension simulated is a real semi-active one i.e. a spring (nonlinear) plus an active actuator. In such a way we explicitly model the fact that the damper is replaced by the actuator. Such a control also justify the choice of $\{k_{fl}, k_{fr}\}$ as varying parameters in the qLPV synthesis.

A. The LTI case

First we show the advantages of the mixed $\mathcal{H}_\infty/\mathcal{H}_2$ compared to \mathcal{H}_∞ synthesis (for the same γ_∞). In this simulation we generate a step road disturbance on the first then on the second wheel, then a roll moment disturbance and we compare controllers performances according to the passive suspension.

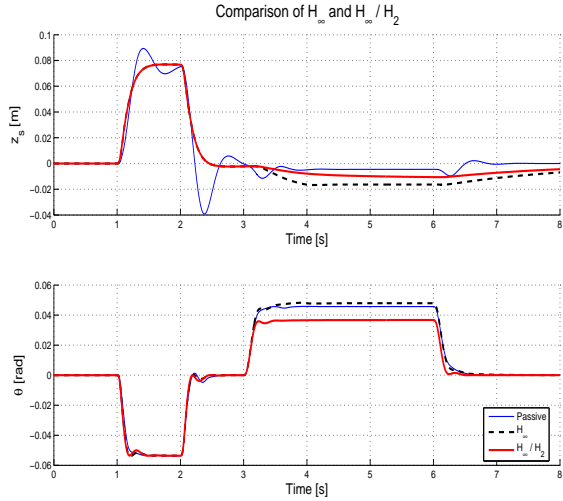


Fig. 6. Comparison between \mathcal{H}_∞ (dashed) and Mixed (solid) design with Passive (solid slim)

By using the mixed synthesis instead of single \mathcal{H}_∞ , we reduce the roll angle due to the roll energy minimization (Figure 6). Then, we compare the performances of the mixed synthesis for different couples $\{\gamma_\infty, \gamma_2\}$ (Figure 7).

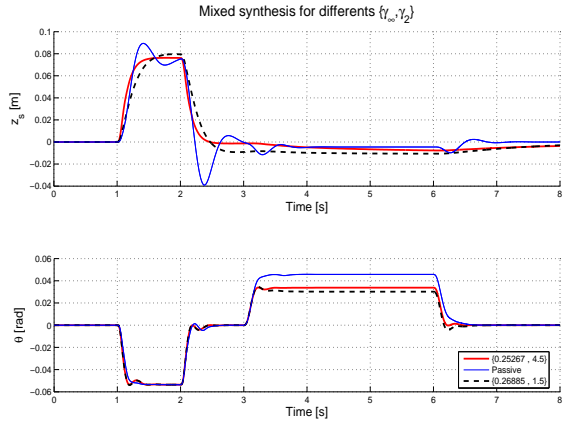


Fig. 7. Comparison of mixed synthesis performances according to different $\{\gamma_\infty, \gamma_2\}$

If one decrease the γ_2 attenuation value, then it increases the γ_∞ one (see Pareto limit Figure 5). The \mathcal{H}_2 criteria's aim is to minimize the energy and variations of a signal (here, z_s but also the control input are limited). Hence we observe that the z_s variations are smoother by using a smaller attenuation gain on the \mathcal{H}_2 criteria (less oscillations, i.e. ameliorate vertical comfort).

B. The qLPV case

LTI and the qLPV controllers are here (Figure 8, 9 and 10) investigated for parameters $k_{\{fl, fr\}}$ varying between $k_{nom} \times [1, 1.95]$ (i.e. $[\underline{k}_{fl, fr}, \bar{k}_{fl, fr}]$) and for a fixed $\gamma_\infty = 0.25$.

Here, we assume bigger road step disturbance to reach the nonlinear area of the suspension deflection.

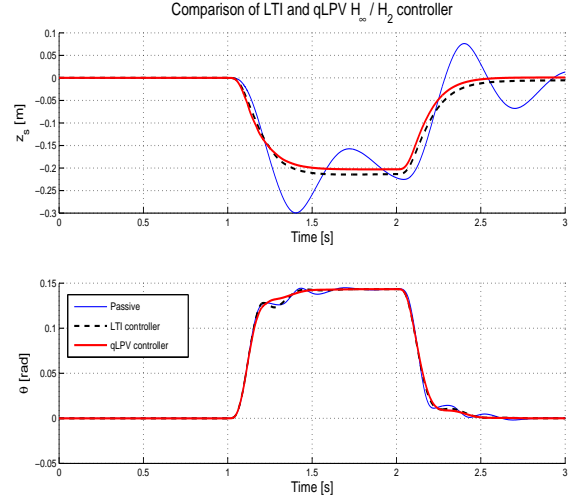


Fig. 8. Comparison of LTI (dashed) and qLPV (solid) mixed synthesis performances

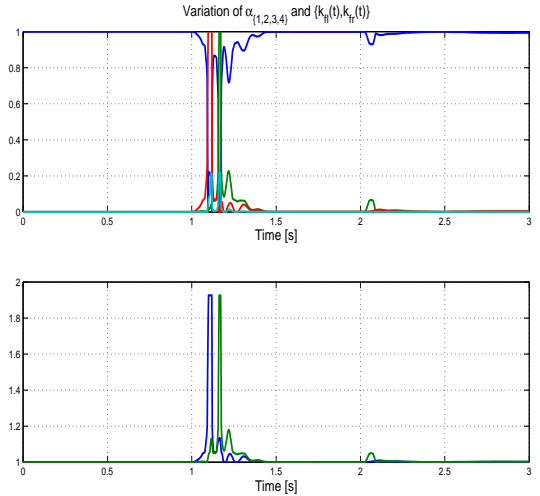


Fig. 9. Variations of $k_{fl} = k_1$ and $k_{fr} = k_2$ (down) and the α (up) computed by the LPV controller

The qLPV synthesis improves the performances achieved by the LTI one. Then, such a control tackle the nonlinearities, hence enforce robustness [15]. The α variations shows the scheduling done according to the parameters variations. Note that a qLPV approach, even if enforces robustness, exhibits more complexity than the LTI one because it increases the number of controllers to be synthesized (4 in our case) and requires to schedule them in real-time. Then, the control signal looks sensitive to the parameters variations (Figure 10). Nevertheless, we use in both synthesis (LTI and qLPV) the same number of measures.

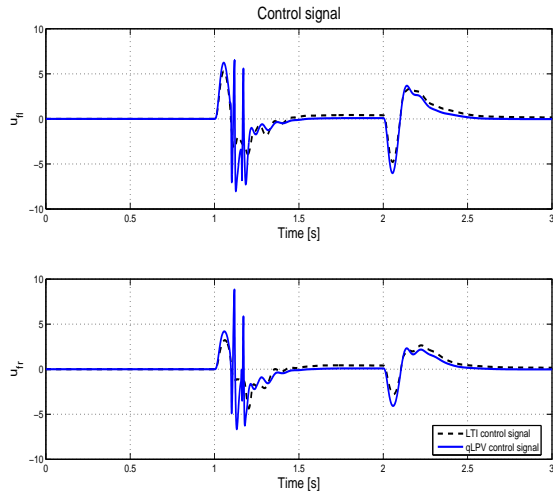


Fig. 10. Control signal u_{fl} (up) and u_{fr} (down) for the LTI (dashed) and qLPV (solid) controller

V. CONCLUSION AND FUTURE WORKS

In this paper we investigate a multi-objective mixed qLPV $\mathcal{H}_\infty/\mathcal{H}_2$ control applied to a half vehicle model. A special interest is made on the advantages of such a synthesis and on the compromises that have to be done in multi-objective applications. By using the Pareto limit (non-inferior solution) we expose a smart way to select the objectives and show the influence on significative driving situations.

In future works we aim to extend the mixed synthesis to a full vehicle model, in a global chassis control framework. Effort have to be made to express precise frequency specifications to each controlled output (roll, pitch...). LPV theory, in the global strategy involving steering and braking actuators, can also be extended to prevent emergency rollover or braking situations [5]. Investigations on polytope reduction (reduce conservatism) should also be explored.

REFERENCES

- [1] E. Abdellahi, D. Mehdi, and M. M Saad. On the design of active suspension system by \mathcal{H}_∞ and mixed $\mathcal{H}_2/\mathcal{H}_\infty$: An LMI approach. In *Proceedings of the American Control Conference*, pages 4041–4045, Chicago, Illinois, USA, june 2000.
- [2] M. Chilali and P. Gahinet. \mathcal{H}_∞ design with pole placement constraints: an LMI approach. *IEEE Transaction on Automatic Control*, 41(3):358–367, march 1996.
- [3] J. C. Doyle, K. Zhou, K. Glover, and B. Bodenheimer. Mixed \mathcal{H}_2 and \mathcal{H}_∞ performance objectives: Optimal control. *IEEE Transaction on Automatic Control*, 39:1575–1587, 1994.
- [4] I. Fialho and G. Balas. Road adaptive active suspension design using linear parameter varying gain scheduling. *IEEE Transaction on Systems Technology*, 10(1):43–54, january 2002.
- [5] P. Gaspar, Z. Szabo, and J. Bokor. The design of an integrated control system in heavy vehicles based on an LPV method. In *Proceeding of the 44th IEEE Conference on Decision and Control*, Seville, Spain, december 2005.
- [6] P. Gaspar, I. Szaszi, and J. Bokor. Mixed $\mathcal{H}_2/\mathcal{H}_\infty$ control design for active suspension structures. *Periodica polytechnica ser. transp. eng.*, 28(1-2):3–16, november 2000.
- [7] P. Gaspar, I. Szaszi, and J. Bokor. Active suspension design using LPV control. In *Proceedings of the 1st IFAC Symposium on Advances in Automotive Control*, pages 584–589, Salerno, Italy, 2004.

- [8] P. Gaspar, I. Szaszi, and J. Bokor. Rollover stability control for heavy vehicles by using LPV model. In *Proceedings of the 1st IFAC Symposium on Advances in Automotive Control*, Salerno, Italy, 2004.
- [9] D. Hrovat. Survey of advanced suspension developments and related optimal control application. *Automatica*, 33(10):1781–1817, october 1997.
- [10] C. Poussot-Vassal, O. Sename, L. Dugard, R. Ramirez-Mendoza, and L. Flores. Optimal skyhook control for semi-active suspensions. In *Proceedings of the 4th IFAC Symposium on Mechatronics Systems*, pages 608–613, Heidelberg, Germany, september 2006.
- [11] D. Sannier, O. Sename, and L. Dugard. Skyhook and \mathcal{H}_∞ control of active vehicle suspensions: some practical aspects. *Vehicle System Dynamics*, 39(4):279–308, april 2003.
- [12] C. Scherer, P. Gahinet, and M. Chilali. Multiobjective output-feedback control via LMI optimization. *IEEE Transaction on Automatic Control*, 42(7):896–911, july 1997.
- [13] C. Scherer and S. Wieland. *LMI in control (lecture support)*. 2004.
- [14] R.H.C. Takahashi, J.F. Camino, D.E. Zampieri, and P.L.D. Peres. A multiobjective approach for \mathcal{H}_2 and \mathcal{H}_∞ active suspension control. In *Proceedings of the American Control Conference*, pages 48–52, Philadelphia, USA, june 1998.
- [15] A. Zin. *Robust automotive suspension control toward global chassis control*. Phd thesis (in french), INPG, Laboratoire d’Automatique de Grenoble, october 2005.
- [16] A. Zin, O. Sename, P. Gaspar, L. Dugard, and J.Bokor. An LPV/ \mathcal{H}_∞ active suspension control for global chassis technology: Design and performance analysis. In *Proceedings of the IEEE American Control Conference*, Minneapolis, USA, june 2006.